Available online at www.sciencedirect.com
SCIENCE DIRECT®
Ultrasonics 43 (2005) 699–709
Ultrasonics
www.elsevier.com/locate/ultras

Mutually induced variations in dissipation and elasticity for oscillations in hysteretic materials: Non-simplex interaction regimes

V.Yu. Zaitsev [a,*], V.E. Gusev [b], Yu.V. Zaytsev [a]

[a] Institute of Applied Physics RAS, 46 Uljanova Street, Nizhny, Novgorod 603950, Russia
[b] Université du Maine, Avenue Olivier Messiaen, 72085, Le Mans Cedex 09, France

Received 13 August 2004; received in revised form 26 October 2004; accepted 21 January 2005
Available online 26 February 2005

Abstract

Self-action and effects mutually induced by oscillations interacting in hysteretic media are investigated analytically and numerically. Special attention is paid to non-simplex processes for which presence of intermediate extrema results in appearance of minor nested loops inside the main hysteretic stress–strain loop. Non-simplex regimes are typical of interaction of excitations having different frequencies and amplitudes, but comparable strain rates. It is found that, due to transition between the regimes, frequency and amplitude dependencies of the variations in elasticity and dissipation induced by one wave for another one may become non-monotonous. Either additional dissipation or induced transparency may occur in different regimes. The results obtained are important for correct interpretation of experimental data on nonlinear acoustic interactions in rocks and many other microstructured (mesoscopic) solids that are known to exhibit elastic hysteresis and memory properties.

PACS: 43.25.Dc; 91.60.Lj; 91.30.-Fn

Keywords: Hysteresis; Wave interaction; Nonlinear dissipation; Induced dissipation; Modulus defect

1. Introduction

Experimental studies of nonlinear self- and inter-action of elastic waves in a wide class of solids (rocks, polycrystalline metals, grainy materials, etc.) indicate manifestations of hysteresis in the stress–strain relationship. For large enough strains (from 10^{-3}–10^{-4} down to $\geqslant 10^{-5}$), direct observations of quasi-static hysteretic loops have been known over 30–40 years [1–5]. For typical acoustic strains $\leqslant 10^{-6}$, such direct observations are not yet available, so that the nonlinear stress–strain relationship has to be reconstructed via comparison of theoretical predictions based on an assumed model(s) with experiments [6–13], although such a reconstruction often is not unique.

For example, in rocks and other microinhomogeneous solids, unlike homogeneous solids possessing weak power-type atomic nonlinearity [14], an important role may belong to manifestations of "non-classical" (and often non-analytical) contact nonlinearity [15–22], together with nonlinear-dissipative [13,16] and slow dynamics phenomena [23,24]. There is also general consensus that, in these solids, the quasi-static hysteresis may be responsible for such effects as nonlinear shift in resonance frequencies accompanied by nonlinear dissipation and higher harmonic generation in resonant-bar experiments at sinusoidal excitation [6–12,25–27]. The recent trend is related to studies of interactions of

* Corresponding author. Tel.: +7 8312 16 48 72; fax: +7 8312 36 59 76.
E-mail address: vyuzai@hydro.appl.sci-nnov.ru (V.Yu. Zaitsev).

0041-624X/$ - see front matter © 2005 Elsevier B.V. All rights reserved.
doi:10.1016/j.ultras.2005.01.005

waves of different frequencies in hysteretic materials [13,21,24,28–35]. The main difficulty in the theoretical description of these effects is related not to the very fact of existence of hysteretic loops, but rather to the property of memory [3,4,36] in a sense that the material response may essentially depend on the history of its deformation. This is especially important for comparable strain rates of interacting excitations, for which hysteretic curves may exhibit multiple nested loops that depend in a rather complex manner on previous extrema in the material loading.

For strong enough difference in the strain amplitudes and rates of the interacting waves, there are no nested hysteretic loops (such processes are called simplex). This case can be treated analytically using the perturbation method. In such a way action of a stronger wave on another weaker one is considered in paper [32]. The opposite influence of a weaker excitation on the stronger one was analyzed in [33]. Recently, an example of a non-simplex interaction of co-propagating waves at fundamental and double-frequency harmonics was considered for quadratic hysteresis with odd symmetry [34,35]. It was found, in particular, that these waves can mutually induce either additional absorption (darkening) or transparency depending on the relative phases and amplitudes.

It should be noted that any hysteretic nonlinearity implies a nonlinear elastic part, which allows for effects of synchronous scattering like in the case of purely elastic nonlinearity. In order to delineate the role of hysteresis, we consider below the interaction of elastic excitations in a volume of a hysteretic material with dimensions smaller than the lengths of interacting waves. This condition excludes spatial accumulation of the scattering effects (taken into account in [32]), but keeps the manifestations of local nonlinear-hysteretic properties of the material. We focus on the effects of induced variations of dissipation/transparency and variations in elasticity for one wave under the action of another wave. Special attention will be paid to features of non-simplex interaction regimes, which practically have not been studied before either analytically or numerically.

2. Model of the hysteretic nonlinearity

Following the terminology of [36] we use as a basis for the analysis the so-called Preisach–Krasnoselsky approach to the description of hysteresis [37,38], which we shall call below the PKM-formalism acknowledging its further development made by Mayergoyz [39]. According to PKM-approach we assume that nonlinear hysteretic contribution to stress σ_{H} can be presented as a linear superposition of the elementary contributions σ_M from individual hysteretic mechanical elements (cracks, microcontact interfaces, dislocations, etc.) embedded into the elastic matrix material:

$$\sigma_{\mathrm{H}}(s) = \sum_M \sigma_M. \tag{1}$$

Here s is the total material strain (in which the contribution of the linear elastic matrix strongly dominates). The individual elements in the PKM-formalism are assumed to switch their stress at certain threshold values of strain s_{o} (“opening”) and s_{c} (“closing”) as shown in Fig. 1 (the plot at the inset). Eq. (1) formally corresponds to the action of the non-interacting mechanical elements in parallel (summation of forces). Note that the hysteretic stress–strain relationship can also be achieved considering a linear superposition of the elementary volume changes (strains) exhibited by the individual elements at certain threshold values of the applied stresses [8,11]. The distribution of the elements over their controlling parameters in terms of either stresses $(\sigma_{\mathrm{o}}, \sigma_{\mathrm{c}})$ or strains $(s_{\mathrm{o}}, s_{\mathrm{c}})$, as in Fig. 1, is called the distribution in the corresponding PKM-space. It was argued in paper [34] that these representations are equivalent when the hysteretic elements, embedded into the near-Hookean (linear) matrix material, induce a small hysteretic correction to the equation of state.

Let us, as is conventionally done [8,36,40,41], consider for individual mesoscopic elements the simplest hysteretic function of a rectangular shape, for which we assume identical variation of threshold stresses $\Delta\sigma = \sigma_{\mathrm{c}} - \sigma_{\mathrm{o}}$ and different threshold strains s_{c} and s_{o} (see inset in Fig. 1). We also admit the conventionally used assumption on instantaneous switching [8,11,39,40]. In order to evaluate the hysteretic correction to the elastic modulus (equal to the derivative $\partial\sigma_{\mathrm{H}}/\partial s = \sum_M \partial\sigma_M/\partial s$) one needs to differentiate the curve plotted in the inset in Fig. 1:

$$\frac{\partial\sigma_M}{\partial s} = \Delta\sigma\Theta(s, s_{\mathrm{o}}, s_{\mathrm{c}}), \quad \Delta\sigma = \sigma_{\mathrm{c}} - \sigma_{\mathrm{o}} > 0, \tag{2}$$

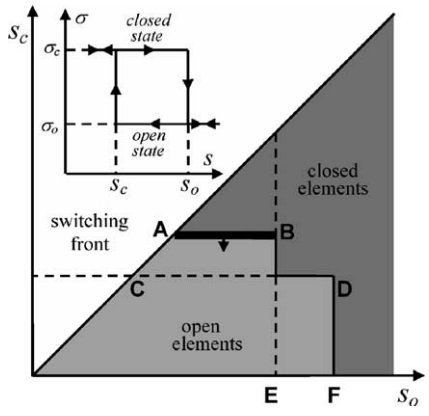

Fig. 1. Hysteretic model of an individual mesoscopic element M (inset) and the PKM-plane $(s_{\mathrm{o}}, s_{\mathrm{c}})$. Each element is parameterized by values of respective strains $s_{\mathrm{o}}, s_{\mathrm{c}}$ corresponding to the element opening and closing, and the variation in the individual stress $\Delta\sigma = \sigma_{\mathrm{c}} - \sigma_{\mathrm{o}}$.

$$\Theta(s,s_o,s_c)=-\begin{cases}\delta(s-s_o), & \text{if } \dfrac{\partial s}{\partial t}>0, \text{ in closed state},\\ \delta(s-s_c), & \text{if } \dfrac{\partial s}{\partial t}<0, \text{ in open state},\end{cases} \tag{3}$$

here $\partial s/\partial t$ is the time-derivative of strain. In order to come to the stress–strain relationship, elementary expressions (2) and (3) for the elastic moduli should be further integrated over strain and summed for the chosen distribution $f(s_c,s_o)$ of the elements in the PKM-space. Since by definition $s_c < s_o$ (see Fig. 1), the hysteretic elements at the plane (s_c,s_o) can be located only below the diagonal $s_c = s_o$. Different material properties may be accounted for by using different $f(s_c,s_o)$, for which $f(s_c,s_o)ds_c ds_o$ is the number (per unit physical volume) of the elements with control parameters belonging to intervals $[s_c, s_c + ds_c]$ and $[s_o, s_o + ds_o]$. Examples of reconstruction of inhomogeneous distributions of the hysteretic elements in order to describe particular forms of hysteretic stress–strain experimental protocols are given e.g. in [42]. However, typically such distributions manifest noticeable inhomogeneity at quite large strains, of the order of 10^{-4} and more, whereas in acoustics of solids typical strains are orders of magnitude smaller, so that for these small strains the distribution function could be approximated by a constant, $f(s_c,s_o) = f_0 = \text{const}$. In such a case it was analytically shown in [43] that, for a simplex quasi-periodical straining with one maximum s_{max} and one minimum s_{min} over a loading cycle, the hysteretic correction σ_H in the equation of state is of an odd-type and is quadratic in strain:

$$\sigma_H=\begin{cases}\sigma_H(s_{max})+\dfrac{h_H E}{2}(s-s_{max})^2, & \dfrac{\partial s}{\partial t}<0,\\ \sigma_H(s_{min})-\dfrac{h_H E(s-s_{min})^2}{2}=\sigma_H(s_{max}) & \\ -\dfrac{h_H E}{2}[(s-s_{min})^2-(s_{max}-s_{min})^2], & \dfrac{\partial s}{\partial t}>0.\end{cases} \tag{4}$$

Here E is the linear elastic modulus (determined by the matrix material), and $h_H = f_0\Delta\sigma/E$ is the characteristic nondimensional parameter of the hysteretic quadratic nonlinearity. In Eqs. (4) the background level of stress is not specified. Indeed, this constant does not affect the shape of the hysteresis loop, which determines physical manifestations of the hysteresis (that is harmonic amplitudes, energy dissipation proportional to the loop area in the $\sigma(s)$ plane, variations of the elastic modulus, etc.). It is convenient to consider the hysteretic stress in the normalized form $\sigma_H/(h_H E) \to \tilde{\sigma}_H$, which we shall use below omitting the tilde. Strain s can be conveniently normalized to some characteristic strain s_{ch} beyond which distribution $f(s_c,s_o)$ cannot be considered as constant, $S = s/s_{ch}$, so that below we limit ourselves to small enough strains $S \ll 1$ for which $f(s_c,s_o) \approx f_0$.

For a non-simplex loading with intermediate extrema the boundary between open and closed elements at the PKM-plane becomes step-wise (Fig. 1 demonstrates one intermediate step-wise "switching front", bold segment AB). Such intermediate steps correspond to branches of minor nested loops inside a bigger loop at the stress–strain plane. Much like a simplex loop the branches of the minor loops are described by Eqs. (4), but s_{max} and s_{min} have the meaning of the respective intermediate extrema. Further, at the moment when a minor step (bold segment AB in Fig. 1) is absorbed by the bigger step (segment CD in Fig. 1) the "switching segment" experiences instantaneous elongation (from length AB to length CD as is clear from Fig. 1). The minor loop at this moment returns to the previous-order hysteresis branch started from the corresponding previous extremum (in other words, the system "memory" about the intermediate maximum, denoted as point E in Fig. 1, is "wiped out" and the further evolution is determined by the higher previous maximum denoted as point F). The larger branch is again described by Eqs. (4) with the extrema appropriately "switched" to the previous values. This switching between the hysteretic branches corresponds to the effect of "memory" for non-simplex processes, which in more details is discussed in [34]. Based on the described principle of matching minor and major hysteretic branches of the form given by Eqs. (4), a numerical code was developed to construct hysteretic stress–strain dependencies for arbitrarily complex strain histories. The code determines all the extrema occurring during the given material straining and constructs the corresponding hysteretic stress–strain dependencies keeping track of the memory effects and nested loops as discussed above (some examples are given in Figs. 2 and 3). Experimental observations of complex hysteresis loops of such a type can be found, for example, in [3,42,44].

A higher-frequency oscillation with strain amplitude A_{HF} may create its own smaller loops only when its strain-rate $\omega_{HF}A_{HF}$ becomes higher than the strain-rate $\omega_{LF}A_{LF}$ in the lower-frequency oscillation at some phases of the period of the slower oscillation, as was argued in [29]. Complex character of straining at high frequency ratio $\omega_{HF}/\omega_{LF} \gg 1$ may occur even for $A_{HF}/A_{LF} \ll 1$, the exact threshold being dependent on the mutual phasing of the oscillations. Indeed, the largest strain-rate amplitude $\omega_{HF}A_{HF}$ of the fast oscillation is required in order to exceed the strain rate of the low-frequency oscillation in the vicinity of its strain-rate extrema $\omega_{LF}A_{LF}$. At this unfavourable for creation of nested loops phasing, the threshold condition is $A_{HF} > (\omega_{LF}/\omega_{HF})A_{LF}$. However, in the special case of creation of nested loops near zeros of the strain-rate in the slow oscillation, much smaller amplitude A_{HF} can suffice. In this case the amplitude of strain rate $\omega_{HF}A_{HF}$ in the high-frequency excitation should be compared

with a characteristic strain rate $\sim \omega_{HF}^{-1} d/dt(dS_{LF}/dt) = (\omega_{LF}^2/\omega_{HF})A_{LF}$ attainable by the low-frequency excitation near its strain-rate zeros during the period of the high-frequency oscillation. Thus the threshold condition for this case is much softer, $A_{HF} > (\omega_{LF}/\omega_{HF})^2 A_{LF}$ (see also [33]). Analytically nested loops can be described in ample details only for simple special cases [33–35]. For arbitrary loading their forms will be found numerically and then used for evaluation of hysteresis-induced effects via the procedure described below.

3. Method of investigation of the interaction

Here we present a few general relations describing in a unified form the effects of self-action as well as the influence of one oscillation on the dissipation and elasticity for another oscillation. Let us consider the material straining of the form

$$S = A\cos\theta + a\cos(n\theta + \varphi) \equiv S_A + S_a, \tag{5}$$

where $\theta = \omega t$ is the nondimensional time and n is the ratio of the frequencies of the two oscillations. We shall limit ourselves to rational n in order to be able to consider the process as periodical and to avoid long-time averaging for incommensurable frequencies. However, we shall consider arbitrary amplitude ratios between the interacting waves. In case of strongly different amplitudes we shall call the stronger and the weaker waves "pump" and "probe" respectively.

For the hysteresis-induced losses ΔW_A and ΔW_a per one oscillation period (for the waves at frequencies ω and $n\omega$, respectively) the following expressions have been derived (see Appendix A and also Refs. [33,34]):

$$\Delta W_A = K_1 \oint \sigma_H(\theta)\, dS_A(\theta), \quad K_1 = \begin{cases} 1/n, & n < 1, \\ 1, & n > 1, \end{cases} \tag{6}$$

$$\Delta W_a = K_2 \oint \sigma_H(\theta)\, dS_a(\theta), \quad K_2 = \begin{cases} 1/n, & n > 1, \\ 1, & n < 1. \end{cases} \tag{7}$$

The integration in Eqs. (6) and (7) is performed over the total period T determined by the oscillation with the lower frequency:

$$T = \begin{cases} 2\pi, & \text{for } n > 1, \\ 2\pi/n, & \text{for } n < 1. \end{cases} \tag{8}$$

Eqs. (6) and (7) are valid for arbitrary phases. For the particular phasing described by Eq. (5), $\sigma_H(\theta) = \sigma_H(A\cos\theta + a\cos(n\theta + \varphi))$, $dS_A = -\sin\theta\, d\theta$ and $dS_a = -n\sin(n\theta + \varphi)d\theta$ in Eqs. (6) and (7). Note that in the case of only one wave (either $a = 0$, or $A = 0$) the expressions for the losses $\Delta W_{A,a}$ have the conventional sense of the area of the hysteresis stress–strain loop.

Similar expressions can be obtained for the hysteresis-induced variations in the velocities (elastic moduli) for each of the waves (see Appendix A):

$$\frac{\Delta E_A}{E} = \frac{K}{\pi A^2} \oint \sigma_H(\theta) S_A(\theta)\, d\theta, \tag{9}$$

$$\frac{\Delta E_a}{E} = \frac{K}{\pi a^2} \oint \sigma_H(\theta) S_a(\theta)\, d\theta, \quad K = \begin{cases} 1, & n > 1, \\ n, & n < 1. \end{cases} \tag{10}$$

Eqs. (6)–(10) will be used below for numerical simulations via direct integration of the stress–strain curves accounting for eventual nested loops. These results will be compared with analytical treatment for the simplex type interaction [32–34] and for some particular situations in complex regimes, which also allowed for analytical investigation.

4. Induced absorption and transparency for two-wave interaction in hysteretic materials

Numerical evaluation of Eqs. (6)–(10) for excitations with incommensurable frequencies requires long averaging over intervals much larger than the periods of beatings of the interacting oscillations. However, main features can be demonstrated using periodical processes (that is using rational parameter n in Eq. (5)), which requires much smaller computation time. As argued above, for the odd-type hysteretic nonlinearity, the higher harmonics generated are of odd orders as well. Therefore, since for even numbers n in Eq. (5) the frequencies of the harmonics do not coincide with frequencies of the initial waves, this ensures that the predicted mutual influence of the oscillations is essentially due to the hysteresis rather than due to the direct nonlinear frequency mixing typical of any elastic nonlinearity. By the same reasons, in order to reliably distinguish for odd numbers n the effect of the hysteresis and the frequency-mixing, we have to consider only the influence of the higher-frequency oscillation upon the lower-frequency one.

In the sections below we limit ourselves to consideration of the quadratic hysteresis described by Eqs. (4) (which correspond to homogeneous density of the PKM-elements for normalized strains $S \ll 1$). The influence of hysteresis saturation at higher amplitudes is readily accounted by the suggested simulation procedure and may essentially modify the results. The discussion of the revealed saturation effects will be published elsewhere.

4.1. Interaction of ω–2ω type

For preliminary testing the numerical code, we start with a particular mutual phasing $\varphi = 0$, frequency ratio

$n = 2$ and the oscillation amplitudes $A = A_1$, $a = A_2$ in Eq. (5):

$$S = A_1 \cos\theta + A_2 \cos(2\theta). \tag{11}$$

For such parameters and for quadratic hysteresis, Eqs. (6) and (7) and Eqs. (9) and (10) can be rigorously evaluated analytically even for a non-simplex straining by properly taking into account the amplitude-dependent displacements of the extrema. Using the calculated energy losses ΔW_i over the period the resultant dissipation for each of the waves may be conveniently characterized by the decrement $D_i = \Delta W_i/(2W_i)$ defined via the maximal accumulated elastic energy $W_i = Es_i^2/2$ in the ith wave. The conventionally used quality factor thus equals to $Q_i = \pi/D_i$.

It is convenient to present the final results in normalized form $D_{1,2} = D_{1,2}/(h_H s^0)$, $A_{1,2} = A_{1,2}/s^0$, and to choose the characteristic strain amplitude s^0 the same as in Eqs. (4): $s^0 = s_{ch}$. Note that for a simplex sinusoidal process with strain amplitude s^0 the decrement D_{simp} determined by the area of the hysteretic loop is $D_{simp} = (4/3)h_H s^0$. The respective expressions for the hysteresis-induced normalized decrements $D_{1,2}$ for the two oscillations in the different regimes have the forms (see also [34])

$$D_1 = (4/3)\begin{cases} A_1\left(1 - \frac{1}{5p^2}\right), & p > 1 \text{ (simplex)}, \\ A_2\left(1 + 2p^2 + \frac{1}{5}p^4\right), & p < 1 \text{ (complex)}, \end{cases} \tag{12}$$

$$D_2 = (4/3)\begin{cases} \frac{8}{5}A_1, & p > 1 \text{ (simplex)}, \\ A_2\left(1 + 7p^2 - p^4 - \frac{3}{5}p^6\right), & p < 1 \text{ (complex)}. \end{cases} \tag{13}$$

Here $p = A_1/4A_2$, and $p = 1$ is the threshold between simplex and complex regimes for the particular phasing (11). A similar procedure of calculating the integrals (9) and (10) yields the following expressions for relative variations $\Delta E_{1,2}/E$ in the elastic moduli (which are denoted for brevity as $DM_{1,2}$ and are also normalized to the factor $h_H s^0$ like the decrements $D_{1,2}$):

$$DM_1 = \begin{cases} A_1, & p > 1 \text{ (simplex)}, \\ A_2\left\{\pi(1+p)^2 + \frac{4}{3}(2+p^2)\sqrt{1-p^2} \right. & \\ \quad \left. - 4p\arccos(p)\right\}/\pi, & p < 1 \text{ (complex)}, \end{cases} \tag{14}$$

$$DM_2 = \begin{cases} A_1, & p > 1 \text{ (simplex)}, \\ A_2\left\{\pi(1+p)^2 + \frac{4}{3}p^2(5-2p^2)\sqrt{1-p^2} \right. & \\ \quad \left. - 4p\arccos(p)\right\}/\pi, & p < 1 \text{ (complex)}. \end{cases} \tag{15}$$

Fig. 2(a) and (b) demonstrates a perfect agreement between the numerically calculated and analytically found nonlinear decrements and the variations in the elastic moduli for the $\cos\theta + \cos(2\theta)$ phasing of the waves, which are plotted as functions of strain amplitudes $A_{1,2}$. Fig. 2(c) shows analogous dependencies on A_2 for other characteristic cases of the mutual wave phasing, for which analytical solutions are not available. The

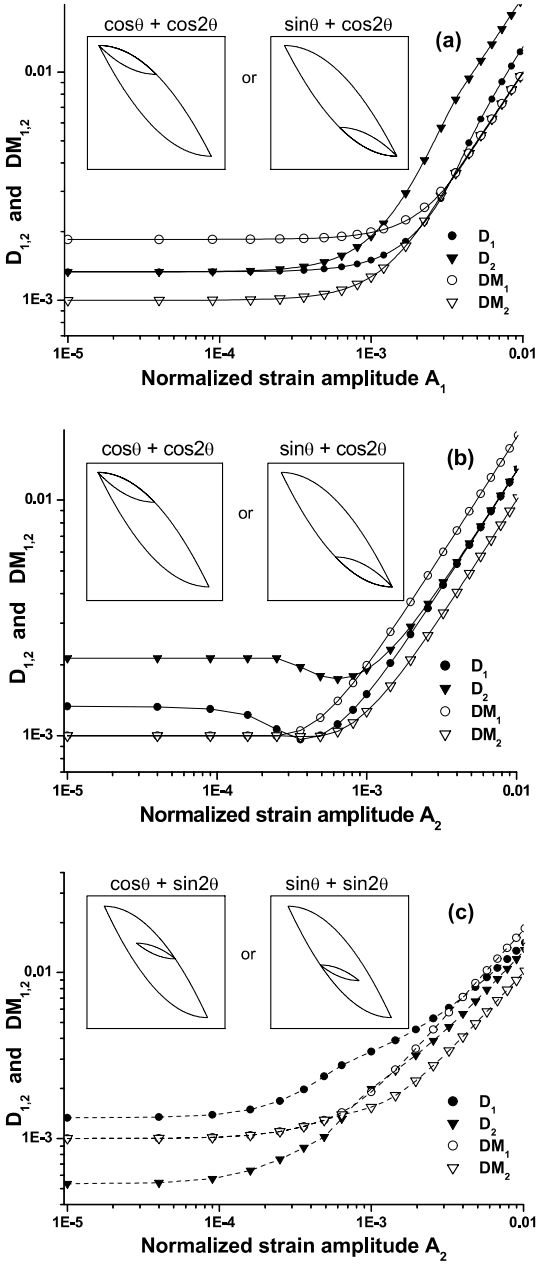

Fig. 2. Nonlinear decrements and modulus defect as functions of amplitudes $A_{1,2}$ for ω–2ω interaction. Insets show nested loops produced by 2ω-wave inside ω-wave hysteresis loop. (a) Variable amplitude A_1 at fixed $A_2 = 0.001$. (b) Variable A_2 at fixed $A_1 = 0.001$. Solid lines at (a) and (b) correspond to analytical result Eqs. (12)–(15). (c) Variable A_2 at fixed $A_1 = 0.001$ for $\cos\theta + \sin2\theta$ and $\sin\theta + \sin2\theta$ phasing. In case (c) unlike case (b) decrements $D_{1,2}$ exhibit no minima in function of A_2.

plots demonstrate that when one wave is much stronger than the other, the induced decrement for the weaker wave is independent on its own amplitude. In this sense the weak-wave losses induced due to nonlinear interaction with the strong wave resemble linear (e.g. viscous) losses, and these losses normally increase with increasing amplitude of the stronger. However, for some phasing (e.g. the cases shown in Fig. 2(b)) the 2ω-wave may induce local minima in the decrements for both waves, which happens in the complex regime for comparable amplitudes of the waves. Note that, in contrast to the dissipation, for the elasticity variations $DM_{1,2}$ the intermediate minima do not exist at any phasing. It should be underlined that the calculated decrements correspond to the "genuine dissipation", in other words, this is the time-averaged irreversible work produced by the strain-actuators for the respective oscillation (in presence of another oscillation). These losses are essentially due to jumping (switching) of the elastic modulus at the end-points of the hysteretic loops. In contrast, in the case of purely elastic nonlinearity the elastic energy in average is conserved inside the material and the two oscillations produce their work independently in average (although the energy is periodically redistributed in reversible way between the fundamental and nonlinearity-induced components). Formally this corresponds to zero value of integrals (6) and (7) (that is zero area contoured by elastically-nonlinear stress–strain curves without splitting over a period).

4.2. Interaction of ω–3ω type

Similar to the considered above, but quantitatively even stronger non-monotonous influence on ω-wave can be produced by a 3ω-oscillation which is capable to create nested loops near both extrema of the ω-wave. As a result, the induced local minimum in the decrement D_1 is deeper than that for interaction with 2ω-wave as is illustrated in Fig. 3 (see also the note on odd frequency ratios in the beginning of Section 4). Moreover, for the "optimal" phasing (sin–sin type interaction) Fig. 3 demonstrates a local minimum for the variation in the elasticity DM_1 as well. It is interesting to check for arbitrary mutual phasing whether the phase-averaged induced transparency for D_1 may persist or not. Fig. 4 shows the influence of the phase shift φ_3 of the interacting ω–3ω waves

$$S = A_1 \cos\theta + A_2 \cos(3\theta + \varphi_3), \tag{16}$$

on the decrement D_1 of the ω-wave. The dashed horizontal line shows the reference magnitude of the self-induced nonlinear dissipation for the ω-wave. This plot indicates that the phase region of the increased dissipation of the ω-wave dominates, so that for ω–3ω interaction the phase-averaged induced transparency cannot be obtained for ω-wave.

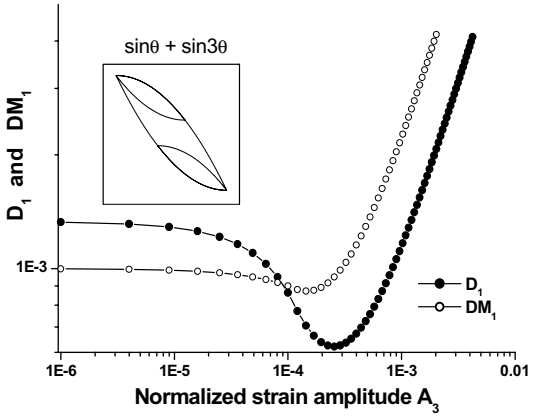

Fig. 3. Decrement D_1 and modulus DM_1 for ω-probe wave with $A_1 = 10^{-3}$ in function of 3ω-pump amplitude A_3 for the phasing when the nested loops are created near the ω-wave extrema. The analogous parameters of the 3ω-wave are not shown, since they are essentially distorted by the direct generation of the 3rd harmonic by the ω-wave.

4.3. Interaction of ω–$n\omega$ type

Let us discuss now the influence of the difference in frequencies between the interacting waves. We again assume the probe wave amplitude A_{pr} to be much smaller than the pump-wave amplitude A_{pm}. In order to avoid the masking effect of directly generated odd-harmonics of the waves we choose even ratios of the frequencies, as was argued above. Fig. 5(a) presents the hysteresis-induced decrements and variations in the elasticity for each of the waves as functions of their relative frequency $\omega_{\mathrm{pm}}/\omega_{\mathrm{pr}}$. It is important that even for a weak probe wave (30 times smaller in amplitude than the pump for Fig. 5(a)) the interaction becomes essentially non-simplex at higher probe-frequency.

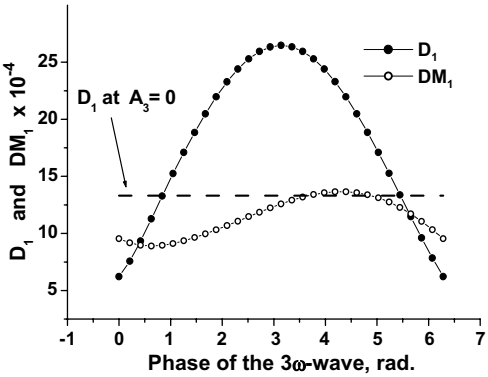

Fig. 4. Dependencies of the induced nonlinear decrement D_1 and modulus defect DM_1 due to interaction with 3ω-wave plotted against the initial phase of the 3ω-wave. Strain amplitudes $A_1 = 10^{-3}$ and $A_3 = 2.6 \times 10^{-4}$ correspond to the minimum of D_1 in Fig. 3. The dashed line shows ω-wave decrement in the absence of 3ω-wave.

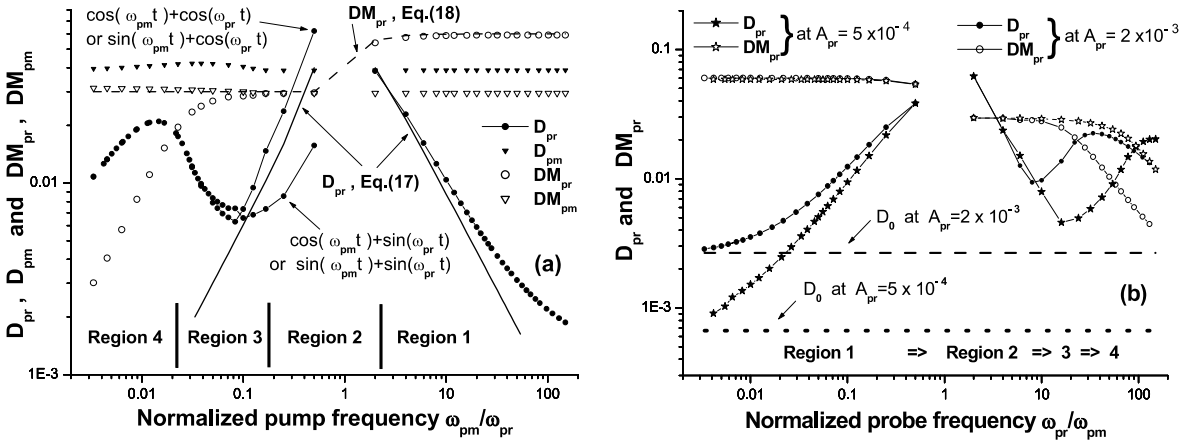

Fig. 5. Nonlinear decrements (filled symbols) and variations in elasticity (empty symbols) plotted against pump and probe wave frequencies for materials with quadratic hysteresis. (a) D_{pr}, D_{pm} and DM_{pr}, DM_{pm} for strain amplitudes $A_{pm} = 0.03$, $A_{pr} = 0.001$ and different mutual phasing against ω_{pm}/ω_{pr}. (b) D_{pr} and modulus defect DM_{pr} for the probe-wave against ω_{pr}/ω_{pm}. Pump amplitude $A_{pm} = 0.03$. Circles are for probe strain amplitude $A_{pr} = 0.002$ and asterisks for $A_{pr} = 0.0005$. Dashed horizontal line corresponds to the probe wave decrement in the absence of the pump for $A_{pr} = 0.002$ and dotted line is for $A_{pr} = 0.0005$.

For such a significant difference in the strain amplitudes, the decrement of the pump wave is determined mostly by its self-action and exhibits only slight variations induced by the probe wave. In contrast, for the probe wave, the dependence of the decrement is essentially determined by the pump-influence and is non-monotonous with qualitatively different behaviour in regions 1–4 in Fig. 5. In regions 1 and 2 both the strain amplitude of the pump and its strain-rate are significantly stronger than those for the probe oscillation, so that the interaction type is simplex as illustrated in Fig. 6 (regions 1, 2). For the high-frequency pump (see Fig. 6 (region 1)), its larger hysteresis loop drifts slowly in the weaker field of the probe wave, but the character of straining remains simplex. Analytically this simplex case of the strong pump was considered in [32]. The numerical results for the lumped interaction can be compared with the case of co-propagating waves at short distance, for which the next approximate expression for the probe wave decrement D_{pr} via the pump strain amplitude A_{pm} follows from [32]:

$$D_{pr} = \frac{2h_H}{\omega_S} A_{pm}\left[1 + \frac{\cos^2(\omega_S \pi/2)}{\omega_S^2 - 1}\right], \qquad (17)$$

where $\omega_S = \omega_{pr}/\omega_{pm}$ in notations [32] for the normalized frequency. Analytical result (17) (see solid lines in Fig. 5(a)) agrees reasonably well with the numerical data for the simplex regime. In region 1 the numerically found probe wave decrement is weakly sensitive to the mutual wave phasing, and well coincides with estimate (17) indicating both quantitative agreement and functionally the same law of the decrease $D_{pr} \propto \omega_{pr}/\omega_{pm}$.

In simplex region 2, the numerical data qualitatively confirm the functional growth $D_{pr} \propto \omega_{pm}/\omega_{pr}$ predicted by Eq. (17), although quantitatively the results in region 2 are more phase-sensitive exhibiting stronger variations around analytical estimate (17) for different wave phasing. For simplex regimes near the transition between regions 1 and 2 it is also essential to point that the probe wave decrement D_{pr} depends mostly on the pump amplitude A_{pm}, but not on the own amplitude A_{pr} of the weaker probe wave. This is confirmed by close values of D_{pr} that are shown in Fig. 5(b) near the transition "region 1 ⇒ region 2" and that are obtained for two different probe-wave amplitudes.

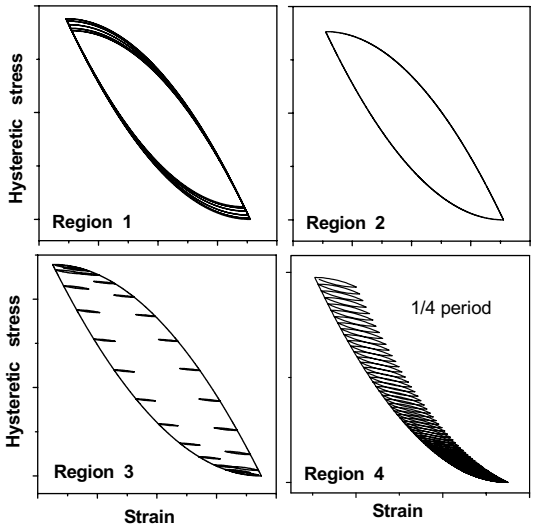

Fig. 6. Shapes of the stress–strain loops for different regimes of the pump-probe interaction corresponding to regions 1–4 in Fig. 6. Amplitude regions 1 and 2 are simplex due to simultaneous large relative strain and large strain rate of the pump. Region 3 is essentially complex even for stronger pump-wave amplitude due to its low strain rate. Region 4 becomes again quasi-simplex for the probe wave, since the pump strain rate is very low (quasi-static pump), and the probe-wave hysteresis loop slowly drifts under the pump action.

Concerning the variations in the elastic moduli, in simplex regions 1 and 2, the numerically calculated values also agree well with the analytical result, which follows from the approach described in [32] for co-propagating waves and has the form similar to (17):

$$DM_{\mathrm{pr}} = -h_{\mathrm{H}} A_{\mathrm{pm}} \left[1 - \frac{1}{\omega_S^2 - 1} \left(\frac{\sin(\pi\omega_S)}{\pi\omega_S} \right) \right]. \qquad (18)$$

After normalization to h_{H} function (18) is shown by the dashed curve in Fig. 5(a). Comparison indicates that this expression coincides well with the numerical data for DM_{pr} shown in Fig. 5(a) (exhibiting, for example, the same 2 times difference between the DM_{pr} magnitudes for the low- and high-frequency pump waves in simplex regions 2 and 1).

For still lower pump frequencies in regions 3, 4 the probe-wave strain rate becomes greater than that of the low-frequency pump, despite much higher strain amplitude of the latter. Therefore, in region 3, the interaction becomes essentially non-simplex, since the probe wave becomes able to create nested loops inside the larger pump-wave loop (see Fig. 6 (region 3)). In the non-simplex region 3, both the induced decrement D_{pr} and the modulus defect DM_{pr} deviate strongly from the analytical estimates (17) and (18). The modulus defect DM_{pr} begins to monotonously decrease in regions 3, 4 for decreasing pump-frequency: $DM_{\mathrm{pr}} \propto \omega_{\mathrm{pm}}/\omega_{\mathrm{pr}}$ (see Fig. 5(a)). In contrast to this monotonous behaviour of the variations in the elasticity, the induced probe wave decrement D_{pr} exhibits non-monotonous dependence. In region 3, the self-induced nested loops for the probe wave result in the intermediate increase of the probe-wave decrement. Physically one may argue that with increase of ratio $\omega_{\mathrm{pr}}/\omega_{\mathrm{pm}}$ (in some range corresponding to region 3) the number of the nested loops increases and the respective probe wave losses also increase. Finally, in region 4, for very low pump frequency the decrement begins to decrease again. In this region the strain-rate in the probe wave is much greater that those in the pump. As a result, the interaction character becomes more simple again, since the shape of the own loops for the probe wave is only weakly affected by the pump wave, and these smaller loops slowly drift under the quasi-static action of the pump as is illustrated in Fig. 6 (region 4). Here the additional pump-induced irreversible work for the probe wave gradually diminishes, so that approximately $D_{\mathrm{pr}} \propto \omega_{\mathrm{pm}}/\omega_{\mathrm{pr}}$. Note also that, in region 4, the pump-induced variation of the decrement for the probe wave is significantly greater than the induced variation in the elasticity, $D_{\mathrm{pr}} \gg DM_{\mathrm{pr}}$, which looks like manifestation of predominantly dissipative nonlinearity.

In Fig. 5(b) we show only probe wave parameters D_{pr} and DM_{pr} in function of the relative probe-wave frequency $\omega_{\mathrm{pr}}/\omega_{\mathrm{pm}}$ for two ratios of the pump- and probe-strain amplitudes. This plot may be considered as a "mirror" plot in frequency domain in comparison with Fig. 5(a), so that the order of regions 1–4 on the frequency axis is inverse. Besides the almost-independence of decrement D_{pr} on the probe wave amplitude in simplex regime (transition between regions 1 and 2), it is interesting to note that frequency dependence of D_{pr} for $\omega_{\mathrm{pm}} > \omega_{\mathrm{pr}}$ resembles the viscous-like case (that is $D_{\mathrm{pr}} \propto \omega_{\mathrm{pr}}$ in agreement with Eq. (17)) and is monotonous. For the relatively low-frequency pump, $\omega_{\mathrm{pm}} \ll \omega_{\mathrm{pr}}$, the frequency behaviour of D_{pr} essentially depends on the ratio of the pump and probe amplitudes and is non-monotonous (much like in Fig. 5(a) near the transition between simplex and non-simplex regimes). The induced decrement D_{pr} can be orders of magnitude greater than the own hysteretic losses for the probe wave (shown by dashed horizontal lines in Fig. 5(b)).

For all examples in Fig. 5 the transition between the interaction regimes is caused by the change of the relative strain-rates due to variation in wave frequencies. Alternatively, for fixed frequencies, the change of the regime evidently could be obtained via varying wave

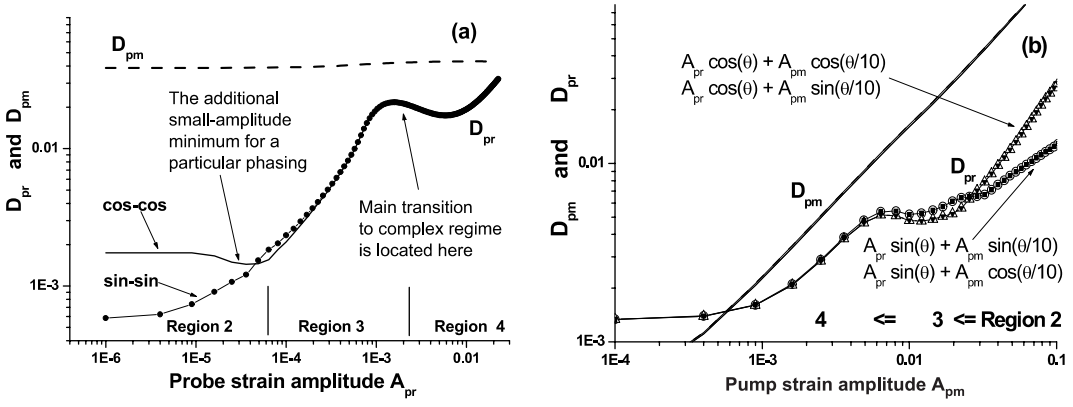

Fig. 7. Examples of amplitude dependencies for nonlinear decrements D_{pm} and D_{pr}. (a) Variable amplitude A_{pr} at fixed $A_{\mathrm{pm}} = 0.03$ for a low-frequency pump $\omega_{\mathrm{pr}}/\omega_{\mathrm{pm}} = 50$. (b) Variable amplitude A_{pm} at fixed $A_{\mathrm{pr}} = 0.001$ for a low-frequency pump $\omega_{\mathrm{pr}}/\omega_{\mathrm{pm}} = 10$. Both dependencies for the probe wave exhibit non-monotonous character much like in Fig. 5.

amplitudes. It may be expected that the resultant non-monotonous behaviour of D_{pr} due to changes in the regimes could be noticeable in the amplitude dependencies as well. The corresponding examples are displayed in Fig. 7(a), in which decrement D_{pr} for the probe wave is plotted as a function of its own amplitude A_{pr} in the case of a relatively strong and low frequency pump. The pump frequency in this example is 50 times lower than the probe frequency and pump strain $A_{pm} = 0.03$ is chosen the same as for Fig. 5. The intermediate maximum (and then minimum) of the probe-wave decrement corresponding to the simplex–complex transition in the interaction regime is clearly visible in the amplitude dependence shown in Fig. 7(a) (much like for frequency-dependencies in Fig. 5). This pronounced non-monotonous behaviour stably occurs for different relative wave phasing near the transition region $3 \Rightarrow 4$, where the probe-wave strain A_{pr} is roughly $\omega_{pm}/\omega_{pr} = 50$ times smaller than the pump-strain amplitude A_{pm}. At such amplitudes at any phasing the probe wave is able to create multiple nested loops over the period of the pump-wave. Due to insensitivity to the phasing these intermediate extrema should persist at incommensurable wave frequencies as well. It is interesting, however, that for certain relative phasing ("cos–cos" case in Fig. 7(a)) there is another intermediate minimum for the probe-wave decrement at much smaller probe-wave amplitudes. This additional minimum appears only at a special phasing, which is favourable for creation of nested loops. For such phasing the transition from simplex to non-simplex regime can manifest itself at much smaller probe wave amplitude $A_{pr} \sim (\omega_{pm}/\omega_{pr})^2 A_{pm}$ (as discussed in the end of Section 2). Note also that, for very small probe strain (in the perfectly simplex regime), the induced decrement D_{pr} is independent on probe amplitude A_{pr}, but in contrast D_{pr} is very sensitive to the relative wave phasing (compare cos–cos and sin–sin cases in Fig. 7(a)). The same phase sensitivity was clearly seen in Fig. 5(a) in simplex region 2.

Finally, Fig. 7(b) presents for the dependence of D_{pr} on the pump amplitude similar features for relatively low-frequency pump, $\omega_{pr}/\omega_{pm} = 10$. However, this frequency ratio is not so big as in Fig. 7(a), so that even the main intermediate minimum exhibits noticeable sensitivity to the wave phasing not only in simplex region 2, but in region 3 as well.

5. Conclusions

The proposed approach allowed us to investigate mutually induced variations in the decrements and elastic moduli for arbitrary ratio of strain- and strain rate amplitudes of oscillations interacting in a hysteretic medium. The simulations indicated that a stronger pump-wave may induce strong additional losses for the weaker wave, which are much greater than its own hysteretic losses. It is essential that, for relatively low-frequency pump-wave, the interaction regime may become non-simplex even at probe-wave strains much smaller than the pump-wave strains. This parameter range is typical, for example, for experiments [28–30] on interaction of pump-oscillations of ~3–10 kHz with ultrasonic probe waves. It is important that the low-frequency pump in the non-simplex regime may induce for the probe-wave additional decrement that is almost an order of magnitude greater than the induced variation in the probe-wave velocity (see Fig. 5, regions 3, 4 with $D_{pr} \gg DM_{pr}$), in contrast to roughly the same order of self-induced variations $D_{pm} \sim DM_{pm}$ for the pump. Such induced effects may look as a manifestation of predominantly dissipative nonlinearity. For high-frequency pump-waves our analysis indicates the inverse situation: pump-induced variations in elasticity for the probe wave could be an order of magnitude larger than the complementary increase in the probe-wave decrement (see Fig. 5(a), region 1).

Frequency dependence of the pump-induced variations for the probe-wave parameters is non-monotonous with strong difference between the cases of high- and low- frequency pump and between simplex–complex regimes. In parameter region 1, the dependence of the probe-wave decrement D_{pr} may be rather smooth in function of both the pump-wave frequency and probe-wave frequency (see Fig. 5). On the other hand, beyond this region the frequency dependence of D_{pr} is non-monotonous (either directly or inversely proportional to pump/probe frequencies respectively to the left or to the right from the wide extrema on the frequency axis as shown in Fig. 5 near the transition between regimes 3 and 4).

Similar non-monotonous features may be seen in the amplitude dependencies for the probe-wave decrement (Fig. 7). In a wide amplitude range (within an order of magnitude) near the transition between simplex and non-simplex regimes 3, 4 the induced decrement D_{pr} may depend rather weakly on both pump- and probe-amplitudes. Besides, decrement D_{pr} for probe-wave with a high accuracy does not depend on its own amplitude in the region of very weak probe-wave amplitudes (see Fig. 7, simplex region 2).

By the order of magnitude the simulated normalized elasticity/decrement variations (Fig. 5) agree satisfactory with some available experimental data indicating comparable magnitudes of the complementary self-induced and mutually induced effects. For example, in [29] the additional decrement for the weaker probe pulses at ~200 kHz under the action of the pump wave at about 3.8 kHz could be estimated as $D_{pr} \sim 0.01$–0.02 with the complementary self-induced variation $DM_{pm} \sim 0.04$ for the elastic modulus, so that ratio DM_{pm}/D_{pr} was about 2–3. The normalized plots presented in Figs. 5

predict a similar magnitude of this ratio in a rather wide range of the probe wave amplitude. More detailed comparison is complicated by the fact that the combined influence of the elastic (reactive) part of nonlinearity together with conventional linear (e.g. thermoelastic or viscous) relaxation may produce similar in magnitude variations in the probe wave decrement, as was mentioned in [29]. Discrimination of these mechanisms using frequency dependencies is not so simple. Indeed, Fig. 5 indicate that the frequency behaviour of $D_{\rm pr}$ essentially depends on the interaction regime (2, 3 or 4), which in its turn depends on the probe wave amplitude at given pump- and probe-wave frequencies. Therefore, simple notion that the probe-wave strain is much weaker than the pump strain is not enough to specify the interaction regime, and calibrated amplitude data are required. For the interacting oscillations belonging to strongly different frequency ranges this is often difficult to provide. In this context, detailed studies of amplitude dependencies (of the type presented in Fig. 7) in a wide strain range at fixed known frequencies could be probably more perspective. Another important point to be taken into account is the influence of saturation of the hysteresis [41], which may essentially modify the discussed above amplitude dependencies for the quadratic hysteresis without saturation.

Acknowledgements

The study was supported by a CNRS contract PECO-NET no. 16366, and the Russian Science Support Foundation and RFBR (V.Z.).

Appendix A. Derivation of integrals for the energy losses and variations in elasticity

We start from the evolution equation for strain S in hysteretic media derived in [41,34]:

$$\frac{\partial S}{\partial x} - \left(\frac{1}{2\rho c_0^3}\frac{\partial \sigma_{\rm H}}{\partial S}\right)\frac{\partial S}{\partial \tau} = 0, \tag{A.1}$$

where $\tau = t - x/c_0$ is the conventionally introduced "running time", and the "reference velocity" $c_0^2 = E/\rho$ is determined by the elastic modulus of the homogeneous solid matrix containing the hysteretic elements (defects). Among the interacting components of the total strain we single out the component with frequency ω, which corresponds to the unit, $n = 1$, frequency for the normalized time $\theta = \omega\tau$:

$$S_1 = A(x)\cos[\theta + \varphi(x)]. \tag{A.2}$$

We are interested to find the variations in the absorption and the elasticity for this component in presence of the other excitations. Let us assume first that the frequency of the other wave(s) is $n > 1$ and consider the nonlinearity-induced variations for the selected wave $A(x)\cos[\theta + \varphi(x)]$. Substituting Eq. (A.2) into (A.1) and singling out explicitly the terms related to the considered wave one gets:

$$\frac{\partial A}{\partial x}\cos(\theta+\varphi) - A\frac{\partial \varphi}{\partial x}\sin(\theta+\varphi) + (\text{components with } n \neq 1) = \left(\frac{\omega}{2\rho c_0^3}\frac{\partial \sigma_{\rm H}}{\partial S}\right)\frac{\partial S}{\partial \theta}. \tag{A.3}$$

Nonlinear term $\frac{\partial \sigma_{\rm H}}{\partial S}\frac{\partial S}{\partial \theta}$ also still contains all the frequencies. Further separation of $\cos(\theta+\varphi)$ and $\sin(\theta+\varphi)$ spectral components in Eq. (A.3) yields:

$$\frac{\partial A}{\partial x} = \frac{1}{\pi}\int_{-\pi}^{\pi}\left(\frac{1}{2\rho c_0^3}\frac{\partial \sigma_{\rm H}}{\partial S}\right)\frac{\partial S}{\partial \theta}\cos(\theta+\varphi)\,{\rm d}\theta, \tag{A.4}$$

$$A\frac{\partial \varphi}{\partial x} = -\frac{1}{\pi}\int_{-\pi}^{\pi}\left(\frac{1}{2\rho c_0^3}\frac{\partial \sigma_{\rm H}}{\partial S}\right)\frac{\partial S}{\partial \theta}\sin(\theta+\varphi)\,{\rm d}\theta. \tag{A.5}$$

For the formulated purpose to investigate the local variations in the absorption and the elasticity, we may put approximately $A(x) \approx A(x=0) = A$ and $\varphi(x) \approx \varphi(x=0) = 0$ unless these variables are differentiated. Taking into account that $\frac{\partial \sigma_{\rm H}}{\partial S}\frac{\partial S}{\partial \theta} = \frac{\partial \sigma_{\rm H}}{\partial \theta}$ and performing integration by parts in Eq. (A.4) we obtain:

$$\frac{\partial A}{\partial x} = \frac{1}{2\pi\rho c_0^3}\int_{-\pi}^{\pi}\sigma_{\rm H}\sin\theta\,{\rm d}\theta = \frac{(-1)}{2\pi A c_0 E}\int_{-\pi}^{\pi}\sigma_{\rm H}\,{\rm d}S_1, \tag{A.6}$$

where modulus $E = \rho c_0^2$ and S_1 is the considered strain-harmonic with frequency ω. Taking into account that $|\partial/\partial\theta| = |\omega c_0 \partial/\partial x|$ this equation may be rewritten as

$$\Delta W_1 \approx 2\pi\frac{\partial W}{\partial \theta} = \int_{-\pi}^{\pi}\sigma_{\rm H}\,{\rm d}S_1, \tag{A.7}$$

where ΔW_1 is the amount of losses (of the elastic energy $W = EA^2/2$ accumulated in the selected harmonic) during one period 2π due to the hysteresis. Thus we recover Eqs. (6) and (7) for the energy losses. Note that for the interaction with lower-frequency harmonics with $n < 1$ the integration period is $2\pi/n$, so that respective factors $K_{1,2}$ appear in Eqs. (6) and (7).

Performing the similar integration in Eq. (A.5) one should take into account that derivative $\partial\varphi/\partial x$ has the meaning of correction Δk to the wave number $k = \omega/c$. The latter relation readily gives $\Delta k/k = -\Delta c/c \approx -\Delta E/(2E)$. Thus, via integration by parts, Eq. (A.5) yields

$$\frac{\Delta E}{E} \approx -\frac{1}{\pi A}\int_{-\pi}^{\pi}\sigma_{\rm H}\cos\theta\,{\rm d}\theta = \frac{1}{\pi A^2}\int_{-\pi}^{\pi}\sigma_{\rm H}S_1\,{\rm d}\theta. \tag{A.8}$$

This equation coincides with Eqs. (9) and (10) in case of interaction with higher harmonics ($n > 1$), and for $n < 1$ the integration period equals to $2\pi/n$, so that corresponding factor $K = n$ appears in Eqs. (9) and (10).

References

[1] N.G.W. Cook, K. Hodgson, Some detailed stress–strain curves for rock, J. Geophys. Res. 70 (12) (1965) 2883–2888.

[2] R.B. Gordon, L.A. Davis, Velocity and attenuation of seismic waves in imperfectly elastic rock, J. Geophys. Res. 73 (1968) 3917–3935.

[3] D.J. Holcomb, Memory, relaxation, and microfracturing in dilatant rock, J. Geophys. Res. 86 (1981) 6235–6248.

[4] G.N. Boitnott, Nonlinear rheology of rock at moderate strains: fundamental observations of hysteresis in the deformation of rock, in: J.F. Lewkowicz, J.M. McPhetres (Eds.), Proc. 15th Annual Seismic Res. Symp., Vail, Colorado, Philips Laboratory of the Air Force Material Command, Handsom Air Force Base, MA, 1993, Environmental Research Papers No. 125, pp. 121–133.

[5] B. McKavanach, F.D. Stacey, Mechanical hysteresis in rocks at low amplitudes and seismic frequencies, Phys. Earth Planet. Interiors 84 (1974) 246–250.

[6] V.E. Nazarov, L.A. Ostrovsky, I.A. Soustova, A.M. Sutin, Nonlinear acoustics of micro-inhomogeneous media, Phys. Earth Planet. Interiors 50 (1988) 65–73.

[7] V.E. Nazarov, Nonlinear acoustic effects in annealed copper, Akust Zhurnal (Sov. Phys. Acoust.) 37 (1991) 150–156.

[8] R.A. Guyer, K.R. McCall, G.N. Boitnott, Hysteresis, discrete memory, and nonlinear wave propagation in rock: a new paradigm, Phys. Rev. Lett. 74 (1995) 3491–3494.

[9] P.A. Johnson, B. Zinszner, P.N.J. Rasolofosaon, Resonance and elastic nonlinear phenomena in rock, J. Geophys. Res. 101 (1996) 11553–11564.

[10] R.A. Guyer, J. TenCate, P. Johnson, Hysteresis and the dynamic elasticity of consolidated granular materials, Phys. Rev. Lett. 82 (1999) 3280–3283.

[11] R.A. Guyer, P.A. Johnson, Nonlinear mesoscopic elasticity: evidence for a new class of materials, Phys. Today 52 (1999) 30–35.

[12] V.E. Nazarov, Amplitude dependence of internal friction in zinc, Acoust. Phys. 46 (2000) 186–190.

[13] V.E. Nazarov, A.V. Radostin, I.A. Soustova, Effect of an intense sound wave on the acoustic properties of a sandstone bar resonator, Exp., Acoust. Phys. 48 (2002) 76–80.

[14] Ch. Kittel, Introduction to Solid State Physics, Wiley Publishers, 1995.

[15] M. Richardson, Harmonic generation at an unbonded interface. I. Planar interface between semi-infinite elastic media, Int. J. Eng. Sci. 17 (1979) 73–85.

[16] R.R. Stewart, M.N. Toksoz, Strain dependent attenuation: observations and a proposed mechanism, J. Geophys. Res. 88 (1983) 546–554.

[17] I.Yu. Solodov, Ultrasonics of non-linear contacts: propagation, reflection, and NDE applications, Ultrasonics 36 (1998) 383–390.

[18] V.Yu. Zaitsev, Nonlindeally packed granular media: numerical modeling of elastic nonlinear properties, Acoust. Phys. 41 (1995) 385–391.

[19] V.Yu. Zaitsev, A.B. Kolpakov, V.E. Nazarov, Detection of acoustic pulses in river sand. Pt. 1. Experiment, Pt. 2. Theory, Acoust. Phys. 45 (1999) 235–241, and 347–353.

[20] V.Yu. Zaitsev, V.E. Nazarov, V.I. Talanov, Experimental study of self-action of seismo-acoustic waves, Acoust. Phys. 45 (1999) 720–726.

[21] V. Zaitsev, V. Gusev, B. Castagnede, Luxemburg–Gorky effect retooled for elastic waves: a mechanism and experimental evidence, Phys. Rev. Lett. 89 (2002) 105502.

[22] V. Tournat, V. Zaitsev, V. Gusev, V. Nazarov, P. Bequin, B. Castagnede, Probing granular media by acoustic parametric emitting antenna: clapping contacts, nonlinear dilatancy and polarization anisotropy, Phys. Rev. Lett. 92 (2004) 085502.

[23] J.A. TenCate, T.J. Shankland, Slow dynamics in the nonlinear elastic response of Berea sandstone, Geoph. Res. Lett. 23 (1996) 3019–3022.

[24] V. Zaitsev, V. Gusev, B. Castagnede, Thermoelastic mechanism for logarithmic slow dynamics and memory in elastic wave interaction with individual cracks, Phys. Rev. Lett. 90 (2003) 075501.

[25] K. Van Den Abeele, P.A. Johnson, R.A. Guyer, K.R. McCall, On the quasi-analytic treatment of hysteretic nonlinear response in elastic wave propagation, J. Acoust. Soc. Am. 101 (1997) 1885–1898.

[26] L. Ostrovsky, P. Johnson, Dynamic nonlinear elasticity in geomaterials, Riv. Nuovo Cimento 24 (2001) 1–46.

[27] V.E. Nazarov, A.V. Radostin, L.A. Ostrovsky, I.A. Soustova, Wave processes in media with hysteretic nonlinearity: Pts 1, 2, Acoust. Phys. 49 (2003) 344–353, and 444–448.

[28] V.E. Nazarov, A.B. Kolpakov, Experimental investigations of nonlinear acoustic phenomena in polycrystalline zinc, J. Acoust. Soc. Am. 107 (2000) 1915–1921.

[29] V.Yu. Zaitsev, P. Sas, Dissipation in microinhomogeneous solids: inherent amplitude-dependent attenuation of a non-hysteretic and non-frictional type, Acustica-Acta Acustica 86 (2000) 429–445.

[30] V.E. Nazarov, Dissipative acoustic nonlinearity of polycrystalline zinc, Acoust. Phys. 47 (2001) 438–447.

[31] K. Van Den Abeele, P.A. Johnson, A. Sutin, Nonlinear elastic wave spectroscopy (NEWS) techniques to discern material damage. Pt I: nonlinear wave modulation spectroscopy (NWMS), Res. Nondestruct. Eval. 12 (2000) 17–30.

[32] V. Gusev, Parametric attenuation and amplification of acoustics signals in the media with hysteretic quadratic nonlinearity, Phys. Lett. A 271 (2000) 100–109.

[33] V. Gusev, V.Yu. Zaitsev, Acoustic dither injection in a medium with hysteretic quadratic nonlinearity, Phys. Lett. A 314 (2003) 117–125.

[34] V. Aleshin, V. Gusev, V.Yu. Zaitsev, Propagation of acoustic waves of non-simplex form in a material with hysteretic quadratic nonlinearity: analysis and numerical simulation, J. Comp. Acoust. 12 (2004) 319–354.

[35] V. Aleshin, V. Gusev, V. Zaitsev, Propagation of initially bi-harmonic sound waves in a 1D semi-infinite medium with hysteretic non-linearity, Ultrasonics 42 (2004) 1053–1059.

[36] I.D. Mayergoyz, Hysteresis models from the mathematical and control theory points of view, J. Appl. Phys. 57 (1985) 3803–3806.

[37] F. Preisach, Über die magnetische Nachwirkung, Z. Phys. 94 (1935) 277.

[38] M. Krasnoselskii, A. Pokrovskii, Systems with Hysteresis, Nauka, Moscow, 1983.

[39] I. Mayergoyz, Mathematical Models of Hysteresis and Their Applications, Elsevier, 2003.

[40] K.R. McCall, R.A. Guyer, Equation of state and wave propagation in hysteretic nonlinear elastic material, J. Geophys. Res. 99 (1994) 23887–23897.

[41] V. Gusev, V. Aleshin, Strain wave evolution equation for nonlinear propagation in materials with mesoscopic mechanical elements, J. Acoust. Soc. Am. 112 (2002) 2666–2679.

[42] R.A. Guyer, K.R. McCall, G.N. Boitnott, L.B. Hilbert, T.J. Plona, Quantitative implementation of Preisach–Mayergoyz space to find static and dynamic elastic moduli in rock, J. Geophys. Res. 102 (1997) 5281–5293.

[43] V.E. Gusev, W. Lauriks, E. Thoen, Dispersion of nonlinearity, nonlinear dispersion and absorption of sound in micro-inhomogeneous materials, J. Acoust. Soc. Am. 103 (1998) 3216–3226.

[44] A.N. Tutuncu, A.L. Polio, A.R. Gregory, M.M. Sharma, Nonlinear viscoelastic behavior of sedimentary rocks, Pt. I: effect of frequency and wave amplitude, Geophysics 63 (1998) 184–194.